Human memory formation is accompanied by rhinal–hippocampal coupling and decoupling

Jürgen Fell[1], Peter Klaver[1], Klaus Lehnertz[1], Thomas Grunwald[1], Carlo Schaller[2], Christian E. Elger[1] and Guillén Fernández[1]

Departments of Epileptology[1] and Neurosurgery[2], University of Bonn, Sigmund-Freud Str. 25, D-53105 Bonn, Germany
Correspondence should be addressed to J.F. (juergen.fell@meb.uni-bonn.de)

Published online: 5 November 2001, DOI: 10.1038/nn759

In humans, distinct processes within the hippocampus and rhinal cortex support declarative memory formation. But do these medial temporal lobe (MTL) substructures directly cooperate in encoding new memories? Phase synchronization of gamma-band electroencephalogram (EEG) oscillations (around 40 Hz) is a general mechanism of transiently connecting neural assemblies. We recorded depth-EEG from within the MTL of epilepsy patients performing a memorization task. Successful as opposed to unsuccessful memory formation was accompanied by an initial elevation of rhinal–hippocampal gamma synchronization followed by a later desynchronization, suggesting that effective declarative memory formation is accompanied by a direct and temporarily limited cooperation between both MTL substructures.

Lesions of certain MTL substructures, most notably of the hippocampus and the parahippocampal region, disturb the declarative memory system, the system that makes memory accessible to conscious recollection[1–4]. Neuroimaging studies suggest that both these MTL substructures participate in memory formation[5–10]. A process in the rhinal cortex, which consists of the histologically distinct entorhinal and perirhinal cortices and is part of the parahippocampal region, precedes a hippocampal process[11]. Anatomically, the perirhinal and parahippocampal cortices provide most of the neocortical input to the entorhinal cortex, which in turn provides the predominant cortical input to the hippocampus via the perforant path[12–14]. However, there is no stringent evidence for a direct interaction between rhinal cortex and hippocampus during declarative memory formation in humans[15]. Moreover, the exact time when such a presumed interaction might take place is unknown.

Phase synchronization of gamma oscillations (electrical brain activity) of around 40 Hz is a general mechanism underlying transient functional coupling of neural assemblies[16,17]. This mechanism provides an explanation for the flexibility and specificity of functional associations between brain modules. Evidence has accumulated that phase coupling of induced (that is, not stimulus-locked) gamma activity is essential in object representation. Different object features processed by distinct neural assemblies are bound together to one coherent percept by synchronized induced activity in the gamma range[18,19]. Long-range association of cortical modules via induced gamma-band coupling subserves the integration of cognitive processes[20–22]. In contrast, the evoked (stimulus-locked) gamma response seems not to be involved in assembly coupling, and its functional role is still unclear[19]. Thus, we analyzed induced gamma synchronization of depth-EEG activity, which was recorded simultaneously from rhinal and hippocampal electrodes in epilepsy patients during a word memorization task. We found successful declarative memory formation to be associated with a transient reduction of gamma power in rhinal and hippocampal recordings together with an initial enhancement of gamma synchronization between both MTL substructures, followed by a later desynchronization.

Results

We took EEG recordings from nine patients with unilateral temporal lobe epilepsy while they performed a single-trial word-list learning protocol with a free recall test after a distraction task. We implanted multicontact depth electrodes bilaterally along the longitudinal axis of each MTL during presurgical evaluation because the zone of seizure onset could not be determined unequivocally by noninvasive investigations[23]. Depth electrodes had a cylindrical surface area of 10 mm^2. Sensitivity is maximal for field potentials generated within the adjacent brain tissue and, in general, decays with the inverse square of the distance[24]. For example, compared to adjacent brain tissue 0.1 mm away from the recording electrode (0.1 mm is the order of magnitude of the thickness of hippocampal layers), a source 1 cm away only contributes 0.01% to the recorded signal. The placement of electrode contacts within the hippocampus and the anterior parahippocampal gyrus, which is covered by rhinal cortex[13], were ascertained by magnetic resonance images in each patient (**Fig. 1**). Only EEG recordings from the MTL contralateral to the zone of seizure origin were analyzed to reduce poorly controllable effects introduced by the epileptic process[25]. Moreover, none of the MTLs investigated here showed any pathology, such as hippocampal atrophy, on clinical MR scans performed during the presurgical work-up. Within these non-epileptic MTLs, we analyzed rhinal and hippocampal recordings with the best signal-to-

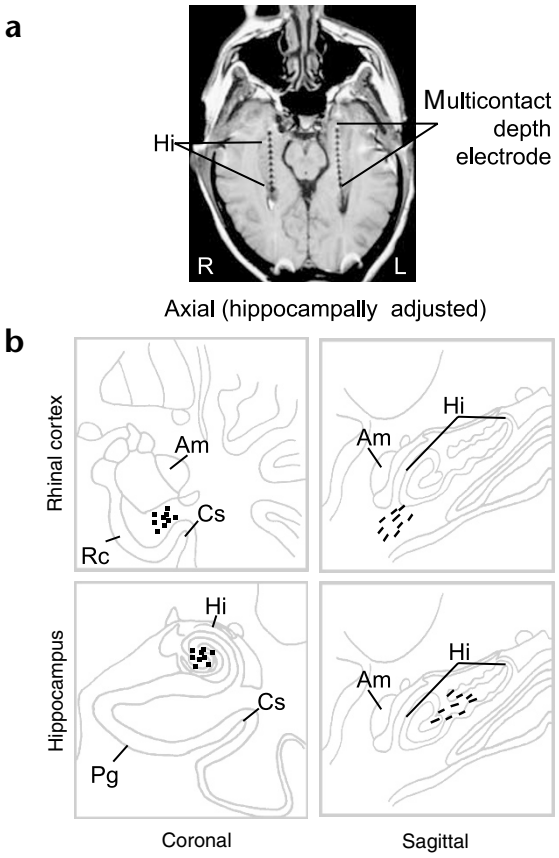

Fig. 1. Localization of MTL depth electrodes. (**a**) Hippocampally adjusted axial MR image of a patient with bilateral depth electrodes *in situ* (Hi, hippocampus; R, right; L, left). Due to MR artifacts, the electrodes appear much larger than their actual size of 1 mm diameter. (**b**) Black dots (coronal) and bars (sagittal) in standardized drawings indicate the approximate location of MTL electrode contacts, which were used to record the EEG tracings analyzed in this study (Am, amygdala; Cs, collateral sulcus; Hi, hippocampus; Pg, parahippocampal gyrus; Rc, rhinal cortex).

noise ratio, assessed by amplitudes of event-related potentials (ERPs) recorded during the same task[11]. The average distance between the selected rhinal and hippocampal locations was 1.6 ± 0.25 cm (mean ± s.e.m.; range, 0.8–2.6 cm).

Each patient participated in 20 study test blocks plus 2 training blocks immediately before the experiment, each containing 12 semantically unrelated German nouns. Patients were instructed to memorize each word presented sequentially on a computer monitor. To prevent ongoing rehearsal, a distraction task was conducted after each block. Thereafter, patients were asked to recall freely the previously displayed words in any order (mean recall rate, 29.7%; range, 20.0–54.6%). In accord with neuropsychological findings in large series of patients with temporal lobe epilepsy[26], memory performance was poorer in the patients investigated here than in healthy subjects performing a similar task[27].

To compare successful and unsuccessful memory encoding, EEG was separated offline into segments for subsequently recalled and unrecalled items. To obtain an optimal time, as well as frequency resolution within the gamma band, we then applied a wavelet technique to the EEG instead of the traditional coherence method. EEG was wavelet-filtered in the gamma frequency range from 32 to 48 Hz (2 Hz steps). Because we investigated induced gamma activity, that is, gamma activity occurring in a non-time-locked fashion in response to the stimuli, analysis was based on single-trial evaluations[19]. Phase synchronization values between electrode contacts within the rhinal cortex and the hippocampus were calculated from the individual wavelet-transformed EEG segments. The higher the synchronization value, the more constant is the phase difference between the two electrodes over all trials. Additionally, averaged power values were determined separately for rhinal and hippocampal recordings for subsequently recalled and unrecalled words. Finally, synchronization and power values were averaged for consecutive 100-ms time windows from –100 ms to 1500 ms relative to stimulus onset.

The time course of phase synchronization between rhinal cortex and hippocampus averaged over all frequencies between 32 and 48 Hz shows a dissociation between subsequently recalled and unrecalled words starting within the first 100 ms after stimulus onset (**Fig. 2**; main effect of time, $F_{14,1008} = 3.47$, $p < 0.001$, $\varepsilon = 0.60$ and interaction of memory × time, $F_{14,1008} = 3.20$, $p < 0.01$, $\varepsilon = 0.50$). Average gamma synchronization between rhinal and hippocampal recordings was increased by up to 16% for subsequently recalled as opposed to subsequently forgotten words from 100 up to 300 ms (main effects of memory, 100–200 ms, $F_{1,72} = 9.39$, $p < 0.005$; 200–300 ms, $F_{1,72} = 3.94$, $p = 0.051$). After the early enhancement in gamma synchronization, a second increase was detected from 500 to 600 ms (main effect of memory, $F_{1,72} = 6.17$, $p < 0.02$) and, finally, a decrease of synchronization was observed from 1000 to 1100 ms (main effect of memory, $F_{1,72} = 6.62$, $p < 0.02$; **Fig. 2**).

The early synchronization effect is most pronounced in the frequency range from 36 to 40 Hz and for these frequencies reaches up to 30% (**Fig. 3**). The second synchronization increase (500–600 ms) and the later desynchronization are prominent in the frequency range from 32 Hz to 40 Hz. Phase lag distributions for both conditions (subsequently recalled and unrecalled words) have a Gaussian shape and are centered around zero (**Fig. 4**). The difference in synchronization for successful and unsuccessful encoding thus arises from a narrowing of the phase lag distribution caused by an increased amount of phase differences close to

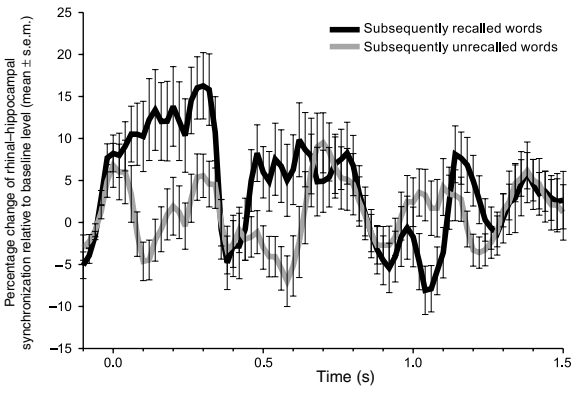

Fig. 2. Changes of phase synchronization between rhinal cortex and hippocampus (%) relative to prestimulus baseline for subsequently recalled versus unrecalled words. Synchronization values were averaged over all analyzed gamma frequencies (32–48 Hz); mean and s.e.m. are plotted. The *x*-axis depicts the time with respect to stimulus onset (word presentation). Time course of synchronization values was calculated from overlapping windows of 100 ms duration shifted in steps of 20 ms.

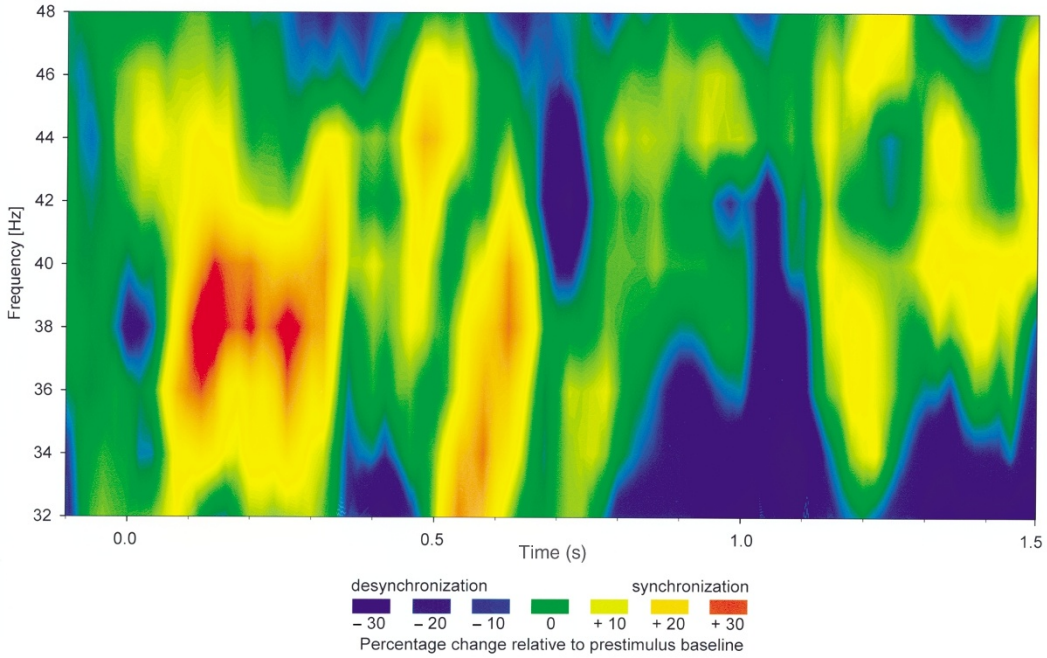

Fig. 3. Differences of phase synchronization between rhinal cortex and hippocampus (%) relative to prestimulus baseline for subsequently recalled versus unrecalled words. Color-coded plot of S(recalled) – S(unrecalled), with S(recalled) = phase synchronization (%) for subsequently recalled words and S(unrecalled) = phase synchronization (%) for subsequently unrecalled words. The different gamma range frequencies (32–48 Hz) are represented in the *y* direction and time is depicted in the *x* direction. Synchronization/desynchronization is coded on a color scale: red areas show an enhancement; blue areas, a reduction of synchronization for subsequently recalled versus unrecalled words.

zero. This finding indicates that rhinal and hippocampal neurons oscillate together in a more synchronous rhythm when encoding leads to successful memory formation.

To explore the possibility that the subsequent memory effects identified here could be related to general, ubiquitous effects found throughout the brain, we examined the synchronization between rhinal cortex and a temporolateral location (gyrus temporalis superior). For identification of the zone of seizure onset, EEG recordings were made from this location with subdural strip electrodes in seven of the nine patients[28]. The two remaining patients had no electrodes outside the MTL. The analysis of rhinal-temporolateral synchronization values revealed neither a memory effect ($F_{1,54} = 1.20$, $p = 0.28$), nor a memory × time interaction ($F_{14,756} = 1.15$, $p = 0.33$, $\varepsilon = 0.63$). Moreover, none of the individual time windows showed a statistically significant memory effect (each $p > 0.05$).

Absolute gamma power values at hippocampal sites were about threefold larger than values from rhinal contacts (average over all frequencies, time windows and conditions, for hippocampus, 39.6 ± 39.8 μV^2; for rhinal cortex, 14.2 ± 12.2 μV^2; paired two-tailed *t*-tests for each individual frequency, condition and time window; all $p < 0.05$, $T_8 > 2.35$). The time course of gamma power at rhinal cortex and hippocampus (**Fig. 5**) dissociated significantly between conditions (ANOVA effects, for rhinal cortex, time ($F_{14,1008} = 14.64$, $p < 10^{-12}$, $\varepsilon = 0.41$) and memory × time ($F_{14,1008} = 4.64$, $p < 0.0001$, $\varepsilon = 0.54$); for hippocampus, time ($F_{14,1008} = 4.68$, $p < 0.0001$, $\varepsilon = 0.62$) and memory × time ($F_{14,1008} = 6.37$, $p < 10^{-7}$, $\varepsilon = 0.59$)). In the rhinal cortex, a gamma peak was observed for both conditions at around 250 ms. However, gamma power was reduced for subsequently recalled compared to unrecalled words (significant reductions from 600 to 800 ms and 1300 to 1400 ms). Similarly, in hippocampal recordings, gamma power was significantly diminished in EEG segments related to successful as opposed to unsuccessful memory formation. This difference was detected between 100 and 400 ms after stimulus onset.

Finally, we compared absolute synchronization and power values for subsequently recalled and unrecalled words during the prestimulus baseline window (–100 to 0 ms) to examine whether EEG changes before word presentation are responsible for our findings, which would have suggested a slowly modulated encoding state rather than transient processes[8]. However, we did not find significant baseline differences between subsequently recalled and unrecalled trials for either rhinal–hippocampal synchronization values ($F_{1,72} = 0.28$, $p = 0.60$), or for gamma power from rhinal ($F_{1,72} = 1.85$, $p = 0.18$) or hippocampal ($F_{1,72} = 1.05$, $p = 0.31$) recordings.

Discussion

Our results show EEG activity in the gamma frequency range in field recordings from within the human MTL during a memory task. A previous study[29] revealed a generally higher gamma power in parahippocampal than neocortical recordings in humans. We extend this knowledge by showing that gamma power in hippocampal recordings is even threefold higher than in the parahippocampal region, suggesting that high-frequency oscillations of around 40 Hz have a prominent involvement in medial temporal and especially hippocampal information processing.

Intracranial EEG recordings allow the reliable separation of synchronization and power effects. In view of the anatomical proximity of the inspected areas (mean distance, 1.6 cm), such a separation would be impossible with surface EEG recordings[30,31]. Previous ERP data indicate[11,32] that there is no detectable correlation between EEG recorded from within the

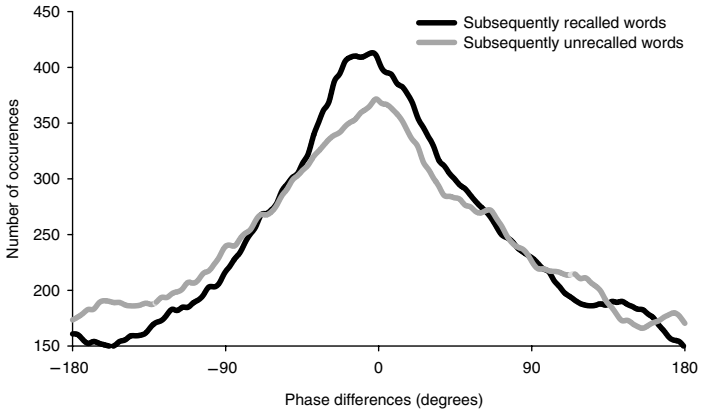

Fig. 4. Distribution of phase differences between rhinal cortex and hippocampus in the gamma frequency range (32–48 Hz) for subsequently recalled versus unrecalled words. Phase differences were evaluated from the time window between 100 and 200 ms after item presentation.

hippocampus and the rhinal cortex, even with electrode distances of less than 1 cm. The large anterior medial temporal lobe N400 component, for instance, which reflects word processing and can be recorded with an amplitude of up to 70 μV from rhinal cortex, is usually not observable in recordings from within the hippocampus[11,27]. On the other hand, hippocampal activity is shielded toward the outside by the radial cylindrical arrangement of hippocampal pyramidal layers[33]. Thus, it is highly unlikely that our results are biased by correlated EEG recordings. We found successful memory formation to be accompanied by two factors: an early increase and a later decrease in gamma synchronization between rhinal and hippocampal recording sites, and a transient reduction of gamma power at both locations partly within the same time window.

The enhancement of gamma-band synchronization observed here between the rhinal cortex and the hippocampus occurs at zero-phase lag. Such a synchronization requires highly accurate timing of neural discharges within a time range of just a few milliseconds[34]. By achieving this, gamma synchronization enables a precise functional association between specific brain regions over short as well as longer distances[16,17]. Thus, gamma-band coupling between rhinal cortex and hippocampus is likely to establish a transient connection between both MTL structures initializing declarative memory formation.

The time course of modulation of gamma synchronization found here is consistent with reports of altered firing rates of single anterior rhinal neurons within 200 ms after visual object presentation[35]. However, it remains unclear whether semantic information provided by each stimulus is already available during the initiation of rhinal–hippocampal coupling or not. If not, directed attention might, in a first step, allocate specific connections necessary for memory formation before actual information transfer takes place. Attention-driven enhancement of gamma-band phase synchronization has been shown in several studies[36–38]. In principle, cortical regions like the prefrontal cortex and the superior temporal sulcus, which are anatomically connected with the MTL, could influence rhinal–hippocampal interaction. The early timing, however, suggests that the observed coupling might be initiated by a top-down process mediated directly by the thalamus[39]. The later decrease in synchronization (1000–1100 ms) may occur following information transfer from the parahippocampal region to the hippocampus[11] and terminate the communication between both structures. Such a functional decoupling has been found in a visual face perception task and has been termed active desynchronization[21].

The timing of rhinal–hippocampal coupling and decoupling fits well with the sequence of processes as monitored by ERPs recorded separately from the rhinal cortex and hippocampus during the same task[11]. Rhinal ERPs in response to subsequently recalled words start to differ from ERPs in response to subsequently forgotten words about 300 ms after stimulus onset. This subsequent memory effect in the rhinal cortex is followed by a hippocampal effect some 200 ms later that lasts until about 2000 ms after stimulus onset. Assuming that rhinal–hippocampal information transfer occurs between the onset of the rhinal and the hippocampal ERP effects, the early beginning of gamma phase coupling revealed here would allow the preparation for and the actual transfer of information. The decoupling observed follows the end of the rhinal subsequent memory effect at about 900 ms after stimulus onset, the time point when information transfer to the hippocampus might be accomplished.

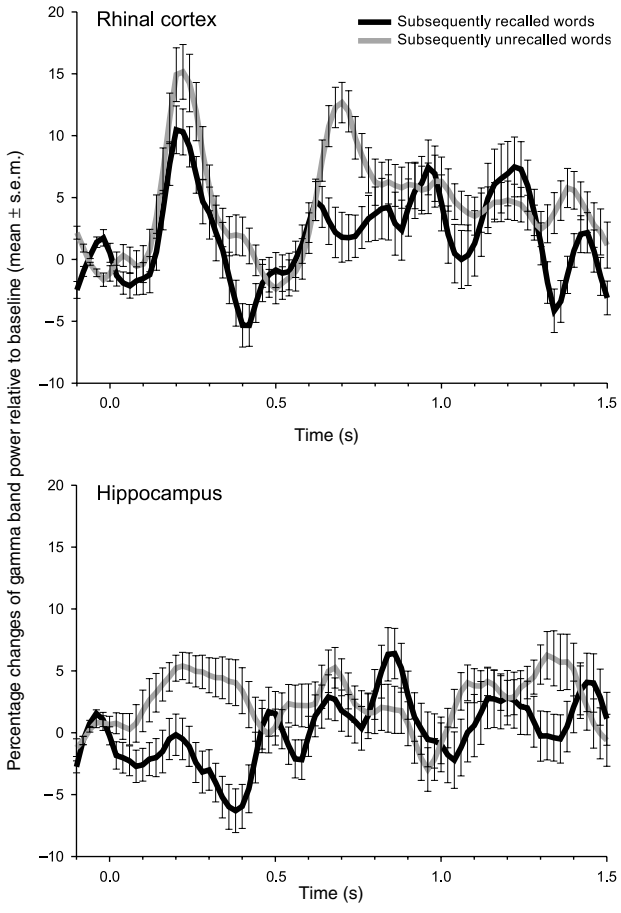

Fig. 5. Changes of EEG gamma power (%) averaged over all frequencies (32–48 Hz) relative to prestimulus baseline for subsequently recalled versus unrecalled words. Mean ± s.e.m. is plotted. The *x*-axis depicts the time with respect to stimulus onset (word presentation).

Gamma oscillations induced in the CA1 field of hippocampal slices within the first second following stimulation are associated with a prolonged elevation of excitatory postsynaptic potentials[40,41], suggesting a crucial involvement in synaptic plasticity, the synaptic correlate of memory formation[42]. These *in vitro* data and our findings underline the importance of medial temporal gamma activity in memory formation. A direct line linking these two sets of data, however, cannot be drawn, as we recorded macroscopic field potentials summing up hippocampal mass activity and were not able to distinguish oscillations generated specifically by distinct hippocampal subregions like the CA1 field.

Our analysis of macroscopic field potentials revealed that efficient medial temporal information processing, leading to successful memory formation, correlates with reduced gamma power at both recording sites. The transient reduction of gamma oscillations might be explained by the necessity to suppress noise-like ambient gamma activity unrelated to specific study items[43]. One might speculate that in an event of unsuccessful encoding, ongoing background gamma activity interferes with item related activity and distorts the process of memory formation. Thus, reduced gamma power, as assessed here during successful encoding, might be a correlate of a higher specificity of local assembly activation. Another interpretation could be that gamma activity behaves like a hippocampal resting rhythm similar to the occipital alpha rhythm. In this picture, certain components of rhinal–hippocampal circuits might be shut off or reset during successful memory encoding.

The results presented here suggest that gamma power reduction and appropriate neural coupling and decoupling interact in declarative memory formation within the human MTL. Our data do not exclude a third pacemaker site driving phase-locked gamma activity in rhinal cortex and hippocampus independently from each other. The strong anatomical connection between both structures[13,14], however, supports the hypothesis of a direct rhinal–hippocampal interaction underlying gamma-band phase coupling and decoupling. Thus, our findings accord with models[11,44], proposing that the formation of new declarative memories requires a direct cooperation between rhinal cortex and hippocampus.

Methods

Subjects. All 9 patients (6 women, 3 men; mean age, 34.1 ± 8.3 years) had pharmacoresistant unilateral temporal lobe epilepsies (mean duration of illness, 26.4 ± 9.1 years). They were native German speakers. At the time of the experiment, all patients received carbamazepine (plasma concentration 8 to 12 μg/ml) as the only centrally acting drug. During presurgical evaluation, at least three spontaneous seizures were recorded invasively using bilateral MTL depth electrodes in all patients and temporo-lateral strip electrodes in seven patients. In six patients, seizures originated exclusively from the right MTL; in three patients, exclusively from the left MTL. No seizure occurred within 24 hours before the investigation. After resection of the epileptic MTL, all patients remained free of seizures (follow-up, 6 to 15 months). In all patients, histopathological examination of tissue resected at the time of epilepsy surgery revealed hippocampal sclerosis. The EEG study was approved by the local medical ethics committee. Each patient gave written informed consent.

Word memorization protocol. Words were presented in uppercase letters for 400 ms. Interstimulus intervals were randomized and ranged from 2.3 s to 2.7 s (mean 2.5 s). Word length ranged from 4 to 11 (mean 6) letters and word frequency ranged from 15 to 175 per million (mean 75 per million)[45]. Patients were asked to use a rote strategy to memorize each word, avoiding memory aids such as making rows, sentences, stories or pictures. During the distraction task, patients were instructed to count backward by threes, starting at a number between 81 and 99 displayed on screen.

EEG recording. Depth electroencephalograms were referenced to linked mastoids, bandpass-filtered (0.03 to 85 Hz, 6 dB/octave), and recorded with a sampling rate of 173 Hz (12-bit analog–digital conversion). To determine the anatomical positions of electrode contacts, MRI scans were acquired in sagittal and adjusted coronal planes, perpendicular to the longitudinal axis of the hippocampus. Electrode contacts were mapped by transferring their positions from MRI to standardized anatomical drawings[46] (**Fig. 1**). EEG trials and corresponding power spectra were visually inspected for artifacts in the gamma frequency range and 4.9% of all trials were excluded from analysis.

Measuring phase synchronization and power. EEG trials were filtered in the gamma frequency range from 32 Hz to 48 Hz (2-Hz steps) by wavelet transforms implementing Morlet wavelets of 7 cycles length. The filtered signals $w_{j,k}$ (j, time point within a trial; k, trial number) hereby result from the time convolution of original signals and the complex wavelet function[47]. From the wavelet transformed signals $w_{j,k}$, the phases $\varphi_{j,k}$ ($\varphi_{j,k} = \arctan(Im(w_{j,k})/Re(w_{j,k}))$) and the power values $P_{j,k}$ ($P_{j,k} = Re(w_{j,k})^2 + Im(w_{j,k})^2$) were extracted for each time point j of each trial k. Power values were averaged separately for trials corresponding to subsequently recalled and unrecalled words. For each time point of each trial, phase differences $\Delta\varphi_{j,k}$ between hippocampal and rhinal electrode contacts were determined. Phase synchronization values S_j were calculated based on the definition of circular variance[48].

$$S_j = \frac{1}{N}\left|\sum_{k=1}^{N} e^{i\Delta\varphi_{j,k}}\right|$$

where N is the number of trials; $S_j \in [0,1]$.

Different numbers of trials for subsequently recalled and unrecalled words would cause a bias in the absolute values of the synchronization measure. Therefore, trial numbers were adjusted between conditions using randomized trial lists for the condition with the originally larger trial number. Finally, power and phase synchronization values were averaged for non-overlapping successive time windows of 100 ms duration from –100 to 1500 ms (16 windows in total).

Statistical analysis. Synchronization and power values were normalized with respect to prestimulus values (window 1) separately for each subject and each filter frequency. For statistical evaluation, we conducted three-way ANOVAs with time (15 windows) and memory (subsequently recalled versus unrecalled) as repeated measures, and frequency (9 levels) as independent variable. p-values were Huynh–Feldt corrected for inhomogeneities of covariance when necessary[49]. The notation of the F-values is $F_{x,y}$ with x being the model degrees of freedom, that is, the number of adjustable parameters in the model, and y being the residual degrees of freedom, that is, the number of degrees of freedom that are not taken up by the model. In a subsidiary analysis, each time window was tested separately by two-way ANOVAs. Effects for time windows with p-values less than 0.05/15 (Bonferroni correction) and for doublets of neighboring time windows each with a p-value less than 0.05 (combined probability less than $0.05^2 \times 14 = 0.035$) were regarded as statistically significant.

Acknowledgements

This research was supported by the Deutsche Forschungsgemeinschaft (DFG Fe479/4-1). We wish to thank H. Beck, W. Burr, A. Engel, C. Koch, M. Reuber and I. Tendolkar for comments on earlier drafts of the manuscript. We also thank H. Urbach for providing the MR images and I. Blümcke for providing the histopathological reports.

Received 12 July; Accepted 10 October 2001

1. Scoville, W. B. & Millner, B. J. Loss of recent memory after bilateral hippocampal lesions. *Neurol. Neurosurg. Psychiatry* **20**, 11–21 (1957).
2. Eichenbaum, H. A cortical-hippocampal system for declarative memory. *Nat. Rev. Neurosci.* **1**, 41–50 (2000).
3. Gabrieli, J. D. E. Cognitive neuroscience of human memory. *Annu. Rev. Neurosci.* **49**, 87–115 (1998).

4. Zola-Morgan, S. & Squire, L. R. Neuroanatomy of memory. *Annu. Rev. Neurosci.* **16**, 547–563 (1993).
5. Otten, L. J., Henson, R. N. A. & Rugg, M. D. Depth of processing effects on neural correlates of memory encoding. *Brain* **124**, 399–412 (2001).
6. Kirchhoff, B. A., Wagner, A. D., Maril, A. & Stern, C. E. Prefrontal-temporal circuitry for episodic and subsequent memory. *J. Neurosci.* **20**, 6173–6180 (2000).
7. Henke, K., Weber, B., Kneifel, S., Wieser, H. G. & Buck, A. Human hippocampus associates information in memory. *Proc. Natl. Acad. Sci. USA* **96**, 5884–5889 (1999).
8. Fernández, G., Brewer, J. B., Zhao, Z., Glover, G. H. & Gabrieli, J. D. Level of sustained entorhinal activity at study correlates with subsequent cued-recall performance: a functional magnetic resonance imaging study with high acquisition rate. *Hippocampus* **9**, 35–44 (1999).
9. Brewer, J. B., Zhao, Z., Desmond, J. E., Glover, G. H. & Gabrieli, J. D. E. Making memories: brain activity that predicts how well visual experience will be remembered. *Science* **281**, 1185–1187 (1998).
10. Wagner, A. D. *et al.* Building memories: remembering and forgetting of verbal experiences as predicted by brain activity. *Science* **281**, 1188–1191 (1998).
11. Fernández, G. *et al.* Real-time tracking of memory formation in the human rhinal cortex and hippocampus. *Science* **285**, 1582–1585 (1999).
12. Lavenex, P. & Amaral, D. G. Hippocampal-neocortical interaction: a hierarchy of associativity. *Hippocampus* **10**, 420–430 (2000).
13. Amaral, D. G. & Insausti, R. in *The Human Nervous System* (ed. Paxinos, G.) 711–755 (Academic, San Diego, 1990).
14. Witter, M. P., Groenewegen, H. J., Lopes da Silva, F. H. & Lohman, A. H. M. Functional organization of the extrinsic and intrinsic circuitry of the parahippocampal region. *Prog. Neurobiol.* **33**, 161–253 (1989).
15. Brown, M. W. & Aggleton, J. P. Recognition memory: what are the roles of the perirhinal cortex and hippocampus? *Nat. Rev. Neurosci.* **2**, 51–61 (2001).
16. Engel, A. K. & Singer, W. Temporal binding and the neural correlates of sensory awareness. *Trends Cogn. Sci.* **5**, 16–25 (2001).
17. Varela, F. J., Lachaux, J.-P., Rodriguez, E. & Martinerie, J. The brainweb: phase synchronization and large-scale integration. *Nat. Rev. Neurosci.* **2**, 229–239 (2000).
18. Sauvé, K. Gamma-band synchronous oscillations: recent evidence regarding their functional significance. *Conscious. Cogn.* **8**, 213–224 (1999).
19. Tallon-Baudry, C. & Bertrand, O. Oscillatory gamma activity in humans and its role in object representation. *Trends Cogn. Sci.* **3**, 151–162 (1999).
20. Singer, W. Striving for coherence. *Nature* **397**, 391–393 (1999).
21. Rodriguez, E. *et al.* Perception's shadow: long-distance synchronization of human brain activity. *Nature* **397**, 430–433 (1999).
22. Miltner, W. H., Braun, C., Arnold, M., Witte, H. & Taub, E. Coherence of gamma-band EEG activity as a basis for associative learning. *Nature* **397**, 434–436 (1999).
23. Van Roost, D., Solymosi, L., Schramm, J., Van Oosterwyck, B. & Elger, C. E. Depth electrode implantation in the length axis of the hippocampus for the presurgical evaluation of medial temporal lobe epilepsy: a computed tomography-based stereotactic insertion technique and its accuracy. *Neurosurgery* **43**, 819–826 (1998).
24. Morris, H. H. & Luders, H. Electrodes. *Electroencephalogr. Clin. Neurophysiol. Suppl.* **37**, 3–26 (1985).
25. Paller, K. A., McCarthy, G., Roessler, E., Allison, T. & Wood, C. C. Potentials evoked in human and monkey medial temporal lobe during auditory and visual oddball paradigms. *Electroencephalogr. Clin. Neurophysiol.* **84**, 269–279 (1992).
26. Hermann, B. P., Seidenberg, M., Schoenfeld, J. & Davies, K. Neuropsychological characteristics of the syndrome of mesial temporal lobe epilepsy. *Arch. Neurol.* **54**, 369–376 (1997).
27. Fernández, G. *et al.* Event-related potentials of verbal encoding into episodic memory: dissociation between the effects of subsequent memory performance and distinctiveness. *Psychophysiology* **35**, 709–720 (1998).
28. Elger, C. E. *et al.* Human temporal lobe potentials in verbal learning and memory processes. *Neuropsychologia* **35**, 657–667 (1997).
29. Hirai, N., Uchida, S., Maehara, T., Okubo, Y. & Shimizu, H. Enhanced gamma (30–150 Hz) frequency in the human medial temporal lobe. *Neuroscience* **90**, 1149–1155 (1999).
30. Menon, V. *et al.* Spatio-temporal correlations in human gamma band electrocorticograms. *Electroencephalogr. Clin. Neurophysiol.* **98**, 89–102 (1996).
31. Bullock, T. H. *et al.* EEG coherence has structure in the millimetre domain: subdural and hippocampal recordings from epileptic patients. *Electroencephalogr. Clin. Neurophysiol.* **95**, 161–177 (1995).
32. McCarthy, G., Nobre, A. C., Bentin, S. & Spencer, D. D. Language-related field potentials in the anterior-medial temporal lobe: I. Intracranial distribution and neural generators. *J. Neurosci.* **15**, 1080–1089 (1995).
33. Klee, M., & Rall, W. Computed potentials of cortically arranged populations of neurons. *J. Neurophysiol.* **40**, 647–666 (1977).
34. Traub, R. D., Whittington, M. A., Stanford, I. M. & Jefferys, J. G. R. A mechanism for generation of long-range synchronous fast oscillations in the cortex. *Nature* **383**, 621–624 (1996).
35. Kreiman, G., Koch, C. & Fried, I. Imagery neurons in the human brain. *Nature* **408**, 357–361 (2000).
36. Steinmetz, P. N. *et al.* Attention modulates synchronized neuronal firing in primate somatosensory cortex. *Nature* **404**, 187–190 (2000).
37. Desmedt, J. E. & Tomberg, C. Transient phase-locking of 40 Hz electrical oscillations in prefrontal and parietal human cortex reflects the process of conscious somatic perception. *Neurosci. Lett.* **168**, 126–129 (1994).
38. Müller, M. M., Gruber, T. & Keil, A. Modulation of induced gamma band activity in the human EEG by attention and visual information processing. *Int. J. Psychophysiol.* **38**, 283–299 (2000).
39. LaBerge, D. Attention, awareness, and the triangular circuit. *Conscious. Cogn.* **6**, 149–181 (1997).
40. Traub, R. D., Whittington, M. A., Buhl, E. H., Jefferys, J. G. & Faulkner, H. J. On the mechanism of the γ_β frequency shift in neuronal oscillations induced in rat hippocampal slices by tetanic stimulation. *J. Neurosci.* **19**, 1088–1105 (1999).
41. Whittington, M. A., Traub, R. D., Faulkner, H. J., Stanford, I. M. & Jefferys, J. G. Recurrent excitatory postsynaptic potentials induced by synchronized fast cortical oscillations. *Proc. Natl. Acad. Sci. USA* **94**, 12198–12203 (1997).
42. Bliss, T. V. P. & Lomo, T. Long-lasting potentiation of synaptic transmission in the dentate area of the anaesthetized rabbit following stimulation of the perforant path. *J. Physiol. (Lond.)* **232**, 331–356 (1973).
43. Craik, F. I. M., Govoni, R., Naveh-Benjamin, M. & Anderson, N. D. The effects of divided attention on encoding and retrieval processes in human memory. *J. Exp. Psychol. Gen.* **125**, 159–180 (1996).
44. Buzsaki, G. The hippocampo-neocortical dialogue. *Cereb. Cortex* **6**, 81–92 (1996).
45. Baayen, R. H., Piepenbrock, R. & van Rijn, H. *CELEX Lexical Database* (Linguistic Data Consortium, University of Pennsylvania, Philadelphia, 1993).
46. Jackson, G. D. & Duncan, J. S. *MRI Neuroanatomy* (Churchill Livingstone, New York, 1996).
47. Daubechies, I. The wavelet transform, time-frequency localisation and signal analysis. *IEEE Trans. Inform. Theory* **36**, 961–1005 (1990).
48. Mardia, K. V. *Probability and Mathematical Statistics: Statistics of Directional Data* (Academic, London, 1972).
49. Huynh, H. & Feldt, L. S. Estimation of the box correction for degrees of freedom from sample data in the randomized plot and split plot designs. *J. Educ. Stat.* **1**, 69–82 (1976).